

# Fatigue Life under Variable Amplitude Loading in a High Strength Steel Showing Step-Wise $S-N$ Curve

M. Nakajima <sup>1</sup>, K. Tokaji <sup>2</sup>, H. Itoga <sup>3</sup> and T. Shimizu <sup>1</sup>

<sup>1</sup> Dept. of Mechanical Engineering, Toyota National College of Technology

<sup>2</sup> Dept. of Mechanical and Systems Engineering, Gifu University

<sup>3</sup> Dept. of Automobile Engineering, Nakanihon Automotive College

**ABSTRACT:** *Fatigue tests under variable amplitude loading were conducted on a high carbon chromium steel, JIS SUJ2. Tests were performed using cantilever-type rotating bending fatigue testing machines in laboratory air. Load sequences employed were two-step block loadings (high→low and low→high) and two-step multiple block loadings (high↔low). Fatigue damages under variable amplitude loading were estimated by the Palmgren-Miner rule. A step-wise  $S-N$  curve was obtained under constant amplitude loading, in which the conventional fatigue limit was about 1275MPa. At stress levels above and below the fatigue limit, the fracture modes were different, i.e. surface-related crack initiation and subsurface crack initiation, respectively. The linear cumulative damage law could evaluate the damages under two-step variable amplitude loadings where the fracture modes were the same, i.e. for subsurface crack initiation. On the other hand, when the fracture mode was different, the cumulative damages,  $\Sigma(n/N)$ , became much larger than unity. Additional fatigue tests were performed using shot-peened specimens to establish the time to subsurface crack nucleation. It was found that the subsurface crack nucleation took place at the early stage of fatigue life.*

## INTRODUCTION

Fatigue damage of machine components subjected to variable amplitude loadings is usually estimated by the linear cumulative damage law proposed by Palmgren [1] and Miner [2]. However, since the effect of stress cycling below the fatigue limit is not considered in the law, fatigue damage can be estimated by means of extending the  $S-N$  curve to lower stress levels, i.e. by the modified Miner rule. Recently, it has been indicated that fatigue failure at stress levels below the conventional fatigue limit occurred in high strength steels, resulting in a step-wise  $S-N$  curve [3-7]. In such a case, since the fatigue lives below the conventional fatigue limit determined experimentally are much longer than the lives assumed by the modified Miner rule, the prediction based on the modified Miner rule overestimates fatigue damage. Although many studies have been conducted under variable

amplitude loadings, studies on steels showing a step-wise  $S-N$  curve are very limited [8,9].

In the present study, giga-cycle fatigue tests under variable amplitude loadings were conducted on a high carbon chromium steel, JIS SUJ2. The results obtained were estimated by the linear cumulative damage law. In addition, the time to subsurface crack nucleation were examined using shot-peened specimens.

## EXPERIMENTAL PROCEDURES

### *Material and Specimen*

The material used was a high carbon chromium steel, JIS SUJ2, whose chemical compositions (mass %) are 1.01C, 0.23Si, 0.36Mn, 0.012P, 0.007S, 0.06Cu, 0.04Ni, 1.45Cr, 0.02Mo and balance Fe.

The material was oil-quenched from 1108K and then tempered for 2h at 453K, from which round bar specimens of hourglass shape with a minimum

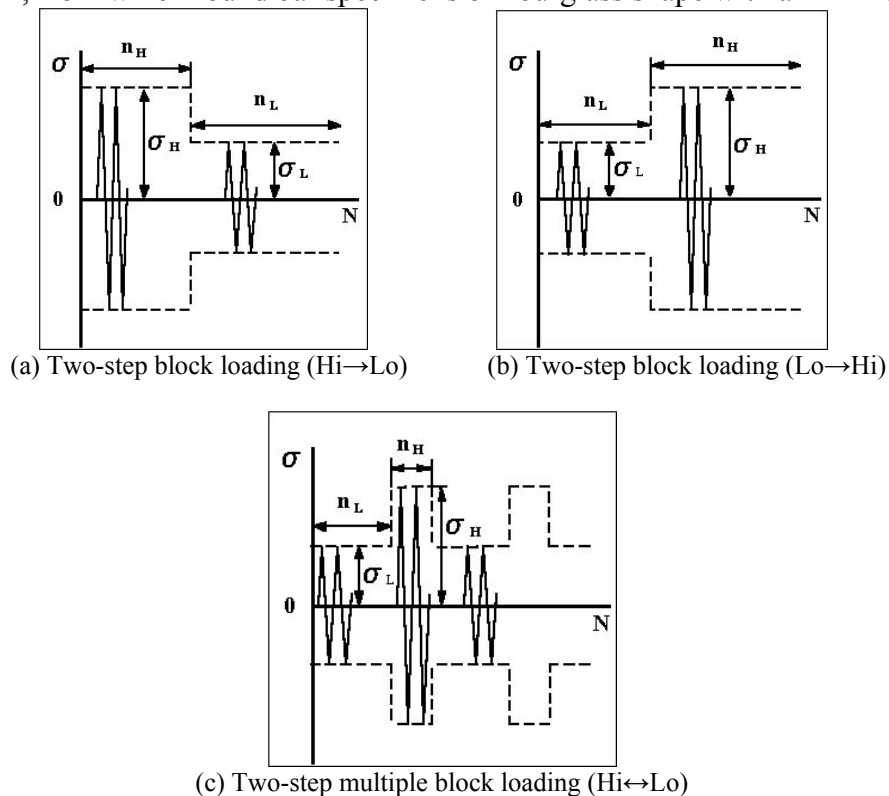


**Figure 1:** Variable amplitude loading patterns.

diameter of 3mm ( $K_t=1.06$ ) were machined. The mechanical properties are as follows; tensile strength  $\sigma_B = 2316\text{MPa}$ , elongation  $\delta=2\%$ , reduction of area  $\varphi=0.4\%$  and Vickers hardness  $HV=778$ .

### ***Fatigue Tests***

Tests were performed using cantilever-type rotating bending fatigue testing machines operating at a frequency of 3150rpm in laboratory air. The run-out stress cycles were fixed at  $1.5\sim 2.0\times 10^9$  cycles. Fracture surfaces of all specimens were examined using a scanning electron microscope (SEM).

Schematic illustrations of variable amplitude loading patterns employed are shown in Fig.1, where (a) and (b) represent the two-step block loadings, Hi→Lo sequence and Lo→Hi sequence, respectively and (c) two-step multiple block loading, *i.e.* Hi↔Lo sequence. Stress levels employed were as follows; the high stress  $\sigma_H = 1100\sim 1600\text{MPa}$  and the low stress  $\sigma_L = 900\text{MPa}$ .

## **RESULTS**

### ***S-N Characteristics under Constant Amplitude Loading***

The *S-N* curves under constant amplitude loading are shown in Fig.2. In this material, fatigue failure occurs at stress levels below the conventional fatigue limit, resulting in a step-wise *S-N* curve. The fracture mechanism operated in higher stress region ( $>1400\text{MPa}$ ) is surface-related crack initiation, while in lower stress region ( $<1100\text{MPa}$ ) subsurface crack initiation with a fish-eye. In the stress range between 1100MPa and 1400MPa, two fracture modes coexist at the same stress level. Therefore, the transition stress at which the fracture mechanism changes from surface to subsurface is present between 1100MPa to 1400MPa.

The conventional fatigue limit was determined by the staircase method, in which the stress interval of 50MPa and the run-out cycles of  $10^7$  were used. The fatigue limit obtained was 1275MPa. In Fig.2, the solid line represents the fitting curve determined by means of the least square method, from which the fatigue lives were obtained, *i.e.*  $N_H$  and  $N_L$  in the Tables 1~4. They were used to estimate the fatigue damages under variable amplitude loading.

The results for the shot-peened specimens were also included in Fig.2. In all the specimens, subsurface fracture was seen regardless of stress level. Therefore, in the region where non-shotpeened specimens showed surface-related fracture, the fatigue lives of the shot-peened specimens are longer

than those of the non-shotpeened specimens. In order to clarify the time to subsurface crack nucleation, additional fatigue tests under variable amplitude loading were performed using shot-peened specimens.

**Results under Hi→Lo Sequence**

The high stress  $\sigma_H=1500\text{MPa}$  and the low stress  $\sigma_L=900\text{MPa}$  were employed. Under constant amplitude loading, surface-related and subsurface fractures occurred at 1500MPa and 900MPa, respectively. The results are listed in Table 1. It has been indicated in a previous study [10] that crack initiation at the surface took place just before failure, thus the number of cycles ( $n_H$ ) at 1500MPa was fixed at almost the same cycles as the fatigue life. After cycling at the high stress, any crack was not detected by optical microscope in three specimens. In addition, the specimens were not failed with the subsequent cycling at the low stress of  $n_L=1.50\times 10^9$ . Therefore, the cumulative damages,  $\Sigma(n/N)$ , became larger than unity.

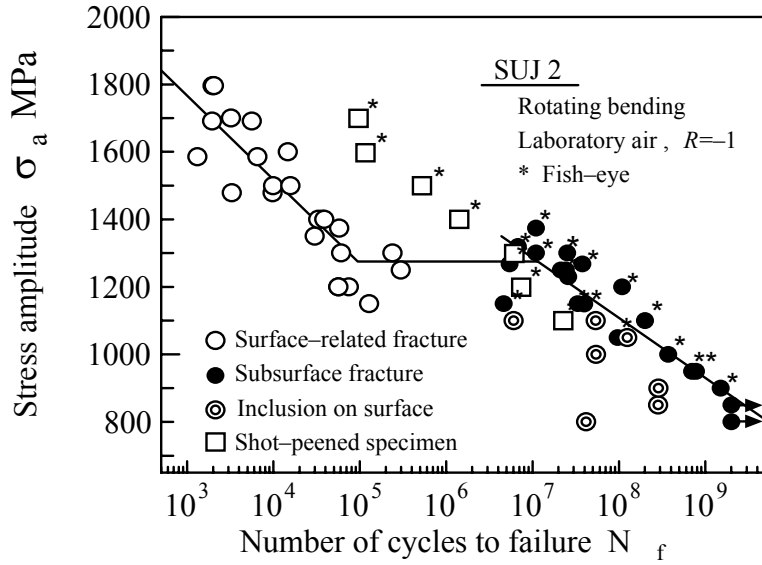


Figure 2: S-N diagram.

TABLE 1: Cumulative damages under (Hi→Lo) variable amplitude loadings

$\sigma_H$ (MPa)	$n_H$	$N_H$	$\sigma_L$ (MPa)	$n_L$	$N_L$	$n_H/N_H$	$n_L/N_L$	$\Sigma(n/N)$
1500	$1.04\times 10^4$	$1.18\times 10^4$	900	$1.50\times 10^9$ (Run-out)	$1.47\times 10^9$	0.88	(1.02)	(1.02)
	$1.19\times 10^4$					1.01		(2.03)
	$1.34\times 10^4$					1.14		(2.16)

### Results under Lo→Hi Sequence

The low stress  $\sigma_L=900\text{MPa}$  and the high stress  $\sigma_H=1100, 1400, 1500$  and  $1600\text{MPa}$  were used. The fracture mode of the high stresses under constant amplitude loading was the surface-related except for  $1100\text{MPa}$ . The number of cycles at  $900\text{MPa}$  was fixed at  $n_L=1.00\times 10^8$  cycles that is about 10% of fatigue life. The results are given in Table 2. The specimens except for the case of  $\sigma_L=1100\text{MPa}$  showed surface-related fracture. Since both  $900\text{MPa}$  and  $1100\text{MPa}$  are below the conventional fatigue limit, the case of  $\sigma_H=1100\text{MPa}$  resulted in subsurface fracture with a fish-eye. As shown in the Table 2, the cumulative damages are considerably larger than unity, *i.e.*  $\Sigma(n/N)=5.67$  at  $1100\text{MPa}$  and about 10 or more at  $1400\sim 1600\text{MPa}$ .

TABLE 2: Cumulative damages under (Lo→Hi) variable amplitude loadings

$\sigma_L$ (MPa)	$n_L$	$N_L$	$\sigma_H$ (MPa)	$n_H$	$N_H$	$n_L/N_L$	$n_H/N_H$	$\Sigma(n/N)$
900	$1.00\times 10^8$	$1.47\times 10^9$	1100	$6.15\times 10^8$	$1.10\times 10^8$	0.07	5.59	5.66
			1400	$4.24\times 10^5$	$2.96\times 10^4$		14.32	14.39
			1500	$1.23\times 10^5$	$1.18\times 10^4$		10.42	10.49
			1600	$5.92\times 10^4$	$4.66\times 10^3$		12.7	12.77

### Results under Hi↔Lo Sequence

The applied stresses were  $\sigma_L=900\text{MPa}$  as the low stress and  $\sigma_H=1100$  and  $1500\text{MPa}$  as the high stress. The fracture modes at  $1100$  and  $1500\text{MPa}$  under constant amplitude loading were the subsurface and the surface-related, respectively. The number of cycles at  $\sigma_L=900\text{MPa}$  in a block was fixed at  $n_L=1.00\times 10^7$  cycles, and the cycles at  $\sigma_H=1100$  and  $1500\text{MPa}$  in a block were  $n_H=2\times 10^6$  cycles and  $1\times 10^3$  cycles, respectively. The results are shown in Table 3. Subsurface fracture was seen in the case of  $\sigma_H=1100\text{MPa}$ , while surface-related fracture in the case of  $\sigma_H=1500\text{MPa}$ . Each fracture mode corresponds to the results under the Lo→Hi sequence shown in Table 2. However, the cumulative damages are small and close to unity.

TABLE 3: Cumulative damages under two-step multiple block loadings

$\sigma_L$ (MPa)	$\Sigma n_L$	$N_L$	$\sigma_H$ (MPa)	$\Sigma n_H$	$N_H$	$\Sigma(n_L/N_L)$	$\Sigma(n_H/N_H)$	$\Sigma(n/N)$
900	$8.20\times 10^8$	$1.47\times 10^9$	1100	$1.64\times 10^8$	$1.10\times 10^8$	0.56	1.49	2.05
	$2.00\times 10^8$		1500	$2.00\times 10^4$	$1.18\times 10^4$	0.14	1.69	1.83

## DISCUSSION

### *The Role of Low Stress Level*

The results given in Tables 1~3 include a stress level below the conventional fatigue limit as the low stress. In the estimation of fatigue damages by the linear cumulative damage law, the role of the low stress is relatively small as considering a step-wise  $S-N$  curve. However, the low stress level led the transition of fracture mode. As described in Table 1, specimens did not fail under Hi→Lo sequence. Using the unbroken specimens, fatigue tests under Lo→Hi sequence were performed. In this case,  $\sigma_L=900\text{MPa}$  and  $n_L=1.50\times 10^9$  cycles in the previous tests was regarded as the loading condition at the low stress, and 1100, 1250 and 1500MPa were applied as the high stress. The results are given in Table 4. All specimens showed subsurface fracture, even in the case of  $\sigma_H=1500\text{MPa}$ . This suggests that the subsurface crack nucleation had already taken place during  $1.50\times 10^9$  cycles at 900MPa, and any fatigue damage did not occur during the first loading at 1500MPa. Furthermore, the fatigue life at 1500MPa, *i.e.*  $n_H=1.54\times 10^6$  cycles, was considerably large compared with the life under constant amplitude loading, because of the occurrence of subsurface fracture.

Based on the results given in Tables 1~4, it seems that the linear cumulative damage law can estimate properly the fatigue damage under two-step variable amplitude loadings where the fracture modes of high and low stresses under constant amplitude are the same, *i.e.* subsurface fracture in the present case. On the other hand, when the fracture modes are different, the cumulative damages become larger significantly than unity.

TABLE 4: Cumulative damages under (Lo→Hi) variable amplitude loadings

$\sigma_L$ (MPa)	$n_L$	$N_L$	$\sigma_H$ (MPa)	$n_H$	$N_H$	$n_L/N_L$	$n_H/N_H$	$\Sigma(n/N)$
900	$1.50\times 10^9$	$1.47\times 10^9$	1100	$1.44\times 10^8$	$1.10\times 10^8$	1.02	1.30	2.32
			1250	$1.52\times 10^7$	$1.58\times 10^7$		0.96	1.98
			1500	$1.54\times 10^6$	$1.18\times 10^4$		130.50	131.52

### *Prediction of Subsurface Crack nucleation*

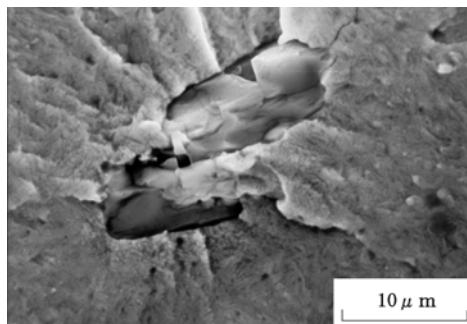
As described previously, the shot-peened specimens showed subsurface fracture regardless of stress level. However, a granular area around non-metallic inclusion was not observed at high stress levels ( $\sigma_H>1400\text{MPa}$ ), as shown in Fig.3(a). Usually, it has been indicated that the granular area was not present at high stress levels [10], even if fish-eye was formed.

Therefore, if a Lo→Hi sequence is applied to the shot-peened specimens, then the time to subsurface crack nucleation would be established by changing the number of cycles at the low stress [9], because the granular area is considered as the initial stage of the fish-eye formation at low stress levels.

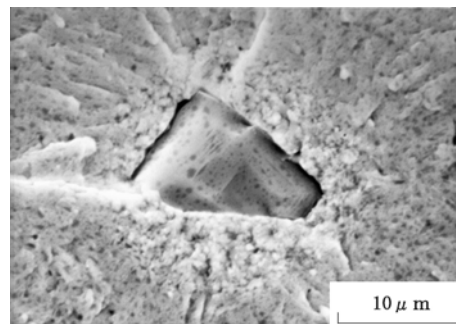
Fatigue tests were carried out at the loading condition of the low stress  $\sigma_L=1100\text{MPa}$  and the high stress  $\sigma_H=1600\text{MPa}$ . The results are listed in Table 5. The number of cycles at 1100MPa was fixed at about 40~90% of the fatigue life. After experiment, fracture surfaces were examined using SEM. The granular area was found in all specimens tested, even at  $(n_L/N_L)=0.37$  as shown in Fig.3(b), which indicates that subsurface crack nucleation takes place at the early stage of fatigue life.

TABLE 5: Cumulative damages under (Lo→Hi) variable amplitude loadings.

$\sigma_L$ (MPa)	$n_L$	$N_L$	$\sigma_H$ (MPa)	$n_H$	$N_H$	$n_L/N_L$	$n_H/N_H$	$\Sigma(n/N)$
1100	$1.00 \times 10^7$	$2.71 \times 10^7$	1600	$2.09 \times 10^4$	$1.79 \times 10^5$	0.37	0.12	0.49
	$1.50 \times 10^7$			$1.04 \times 10^5$		0.55	0.58	1.13
	$2.00 \times 10^7$			$3.47 \times 10^4$		0.74	0.19	0.93
	$2.50 \times 10^7$			$1.07 \times 10^4$		0.92	0.6	1.52



(a) Inclusion and surroundings in fish-eye observed at 1600MPa.



(b) Inclusion and granular area formed at  $\sigma_L=1100\text{MPa}$ .

Figure 3: Microscopic views of inclusion and granular area.

## CONCLUSIONS

Giga-cycle fatigue tests under variable amplitude loadings were conducted on a high carbon chromium steel, JIS SUJ2. The fatigue damages were

evaluated by the linear cumulative damage law and the fracture mechanisms were discussed. The conclusions obtained are as follows;

(1) A step-wise *S-N* curve was seen under constant amplitude loading, in which the conventional fatigue limit was about 1275MPa. At stress levels above and below the fatigue limit, the fracture modes were the surface-related and the subsurface crack initiation, respectively.

(2) The linear cumulative damage law could estimate properly the fatigue damages under two-step variable amplitude loadings where the fracture modes at both high and low stress levels under constant amplitude were subsurface crack initiation, while when the fracture modes were different, the cumulative damages became considerably larger than unity.

(3) Based on the results under variable amplitude loading using shot-peened specimens that showed subsurface fracture regardless of stress level, it was confirmed that subsurface crack nucleation took place at the early stage of fatigue life.

## REFERENCES

1. Palmgren, A., (1924) *V. Deut. Ingenieure*, **68**, 339.
2. Miner, M.A., (1945) *J. Appl. Mech*, **12**, A-159.
3. Emura, H. and Asami, K., (1989) *Trans. Japan Soci. Mech. Eng.*, **55**, 45. (in Japanese)
4. Kuroshima, K., Ikeda, T., Harada, M. and Harada, S., (1998) *Trans. Japan Soci. Mech. Eng.*, **64**, 2536. (in Japanese)
5. Bathias, C., (1999) *Fatigue Fract. Engng Mater. Struct.*, **22**, 559.
6. Murakami, Y., Nomoto, T. and Ueda, T., (1999) *Fatigue Fract. Engng Mater. Struct.*, **22**, 581.
7. Nishijima, S. and Kanazawa, K., (1999) *Fatigue Fract. Engng Mater. Struct.*, **22**, 601.
8. Sugeta, A., Uematsu, Y. and Jono, M., (2001) In: *Proc. of the Int. Conf. on Fatigue in the Very High Cycle Regime*, pp.325-332, Stanzl-Tschegg, S. and Mayer, H., (Eds).
9. Lu, L.T. and Shiozawa, K., (2001) *Proc. of Japan Soci. Mech. Eng.*, **No.01-1, vol.1**, 175. (in Japanese)
10. Nakajima, M., Sakai, T. and Shimizu, T., (1999) *Trans. Japan Soci. Mech. Eng.*, **65**, 2504. (in Japanese)